

Knowledge-Based 3D Segmentation and Reconstruction of Coronary Arteries Using CT Images

Yan Yang, Allen Tannenbaum, Don Giddens

Wallace H. Coulter Department of Biomedical Engineering
Georgia Tech and Emory University, Atlanta, GA 30332

Abstract—An approach for the 3D segmentation and reconstruction of human left coronary arteries using angio-CT images is presented in this paper. Each voxel in the 3D dataset is assumed to belong to one of the three homogeneous regions: blood, myocardium, and lung. A priori knowledge of the regions is introduced via Bayes' rule. Posterior probabilities obtained using Bayes' rule are anisotropically smoothed, and the 3D segmentation is obtained via MAP classifications of the smoothed posteriors. An active contour model is then applied to extract the coronary arteries from the rest of the volumetric data with subvoxel accuracy. The geometric model of the left coronary arteries obtained in this work may be used to provide accurate boundary conditions for hemodynamic simulations, or to provide objective measurements of clinically relevant parameters such as lumen sizes in a 3D sense.

Index Terms—Active contours, Bayes' rule, computerized tomography (CT), coronary arteries, segmentation

I. INTRODUCTION

In this paper we present an approach for segmenting human left coronary arteries using computerized tomography (CT) images. The conventional way of imaging coronary arteries is by using invasive coronary angiography, but effective as it is, this technique brings complicated clinical procedures and risks to the patient. With the development of CT imaging, more details of anatomical structures can be observed, and CT is being considered as an attractive alternative for imaging coronary arteries. The advantages of CT are clear because as a non-invasive imaging technique, it also provides information of the whole 3D volumetric data with high resolution (isotropic voxels on the order of 0.5mm) rather than 2D projections in conventional angiography.

With the 3D volumetric data at hand, it is certainly useful to reconstruct a geometric model and create a 3D view of the coronary arteries. By using contrast enhancing agents, regions filled with blood exhibit higher intensities in CT images, which provide the possibility of extracting these regions from the rest of the given image. In some recent papers, CT images have been used to build geometric models of carotid arteries [1] and cerebral arteries [2]. They also have been used to track the central axis of coronary arteries [3]. The segmentation of

coronary arteries is challenging because coronary arteries are narrow tubular structures winding in-between and around heart chambers with branchings and complex curvatures, and due to the large size of image data, a fast and accurate segmentation approach is desired.

In this work, we first use a knowledge-based segmentation algorithm, analogous to what has been used to segment SAR data [4] and MRI brain images [5] based on Bayes' rule to classify the volumetric data into three homogeneous regions, and find the region that filled with blood (this region includes aorta, pulmonary trunk, heart chambers, and coronary arteries). An active contour model is then applied on the results of the first step, to extract the coronary arteries and obtain a 3D geometric model of the coronary arteries with subvoxel accuracy. The method is described in Section II, and the results are presented in Section III and discussed in Section IV.

II. METHODOLOGY

A. Region Probability Estimation and Region Classification

With the assumption that only three regions - blood-filled region, myocardium region, and lung region - exist in the images, we first roughly cluster the voxels of the 3D volumetric data and learn the mean value (μ_c) and the standard deviation (σ_c) of each class. This can be done via a k-means clustering method, where the voxels are first split into two groups and the one with a larger standard deviation is further split into two other groups. Then the probability density functions can be approximated using Gaussian functions with the learned mean values and standard deviations in each class, which implies that the likelihood of a particular voxel having a certain intensity value v given that it is in class $c \in \{\text{blood, myocardium, lung}\}$ is

$$Pr(V(\mathbf{x}) = v | \mathbf{x} \in c) = \frac{1}{\sqrt{2\pi}\sigma_c} \exp\left(-\frac{(v - \mu_c)^2}{2\sigma_c^2}\right), \quad (1)$$

where $V(\mathbf{x})$ is the intensity value of the voxel at position $\mathbf{x} = (x, y, z)$. We assume that the prior probability that a particular voxel will belong to a certain class (blood, myocardium or lung) is equal and homogeneous, i.e., $Pr(\mathbf{x} \in c)$ is the same for each class and for all voxels. We can then apply the Bayes'

This work is supported by grants from NIH, NSF, and AFOSR.

rule to calculate the posterior probability that a given voxel belongs to a particular class, given its intensity:

$$Pr(\mathbf{x} \in c | V(\mathbf{x}) = v) = \frac{Pr(V(\mathbf{x}) = v | \mathbf{x} \in c) Pr(\mathbf{x} \in c)}{\sum_{\gamma} Pr(V(\mathbf{x}) = v | \mathbf{x} \in \gamma) Pr(\mathbf{x} \in \gamma)} \quad (2)$$

The classification of the voxels is then obtained using the *maximum a posteriori* (MAP) probability estimation:

$$C(\mathbf{x}) = \arg \max_{c \in \{\text{blood}, \text{myocardium}, \text{lung}\}} Pr^*(\mathbf{x} \in c | V(\mathbf{x}) = v), \quad (3)$$

where $C(\mathbf{x})$ is the class that voxel \mathbf{x} belongs to, and Pr^* is a smoothed version of the posterior probability obtained using the anisotropic smoothing [6] described by the following affine invariant flow:

$$\frac{\partial Pr}{\partial t} = \text{sign}(H) \kappa_+^{1/4} \vec{N}, \quad (4)$$

where H and κ are the mean curvature and Gaussian curvature of Pr , and $\kappa_+ := \max\{\kappa, 0\}$. \vec{N} is the inward unit normal. Fig. 1 shows an example of the smoothed posterior probabilities of blood, myocardium and lung in a cross-sectional slice of the volumetric data. Fig. 2 (b) shows the MAP labels of the classification result of this slice, with white corresponding to the blood, gray to the myocardium and dark to the lung.

B. Extraction of the Coronary Arteries: Active Contours

After we have obtained a classification of the 3D data, we can create the binary data by setting the blood-filled region to nonzero and the other two regions to zero. At this point we want to extract the coronary arteries and discard the other blood-filled regions, such as the aorta and the heart chambers. This can be done by running a bubble-growing algorithm starting from the root of the coronary arteries, namely the geodesic active contour models. This model has been described thoroughly in literature (e.g., [7], [8], [9]), and we simply give the level set version of the governing equation used here, which is:

$$\frac{\partial \Psi}{\partial t} = \phi \|\nabla \Psi\| \left(\text{div} \left(\frac{\nabla \Psi}{\|\nabla \Psi\|} \right) + \nu \right) + \nabla \phi \cdot \nabla \Psi, \quad (5)$$

where $\Psi(x, y, z, t)$ is the level set function of the propagating surface, and ϕ is a stopping term that slows down the surface evolution when near an edge. ν is an inflationary constant that determines the direction and speed of the evolving surface. The final surface can be obtained from the zero-level set of Ψ .

Since we are applying the flow to binary data, the method is fast and robust, and it can effectively trace the coronary arteries and extract them from the rest of the data. The only site that could be problematic is the place where the left main (LM) coronary artery bifurcates from the aorta, and the propagating surface may leak into the aorta. This can be prevented by adjusting the weight between the curvature and the inflationary constant in (5), or by manually cutting the linking sites of the LM and the aorta in a few slices of the data where the linkage exists, and evolve the surface solely inside the coronary tree. Fig. 2 (c) shows the segmented blood-filled region using the

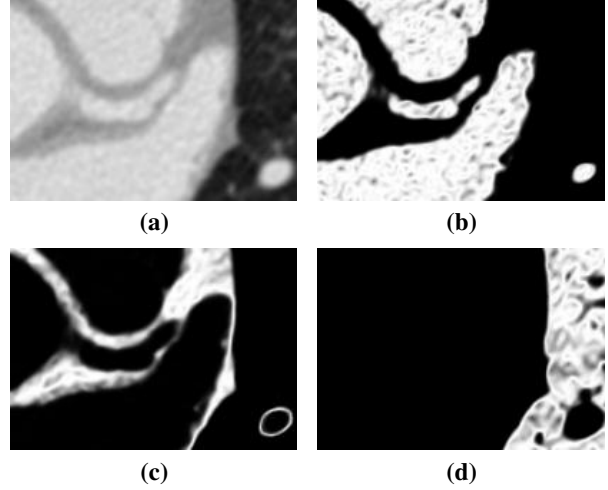


Fig. 1. Smoothed posterior probabilities of a cross-sectional slice. (a) The original gray scaled image. (b)-(d) Smoothed posterior probabilities of blood, myocardium and lung respectively.

MAP classifications with marked white boundaries, and Fig. 2 (d) is the segmented LM coronary artery using active contours based on what is shown in (c).

III. RESULTS

We tested our algorithm on a 3D CT data set of cardiac images. The images were acquired using a GE Lightspeed16 CT scanner with a slice spacing of 0.625mm and a in-plane resolution of 0.6mm. The person being imaged was a normal female volunteer without any clinical heart problems. The original data had a size of $512 \times 512 \times 209$, and the images were cropped to focus on coronary arteries and interpolated to achieve better coherency in the three spacial directions.

By applying the methods described in Section II to this data set, we obtained a 3D model of the left coronary arteries, and the 3D rendering of the model is shown in Fig. 3. In this figure, the LM coronary artery, the left anterior descending (LAD) coronary artery and the left circumflex (LCX) coronary artery are segmented and reconstructed in 3D. Moreover, the first bifurcation of the LAD is also captured and a long section of its branches are captured at the same time.

IV. DISCUSSION AND FUTURE WORK

In this work we proposed a method for segmenting and reconstructing human left coronary arteries in 3D, and we tested the method on a data set of cardiac CT images. The 3D geometric model of coronary arteries can provide a comprehensive view of the vessels, thus helping to achieve more accurate clinical diagnoses. The model can also be used to provide boundary conditions for CFD (Computational Fluid Dynamics) simulations of blood flow and find out the relation between wall shear stress distribution and atherogenesis. This has been done and described in another note [10].

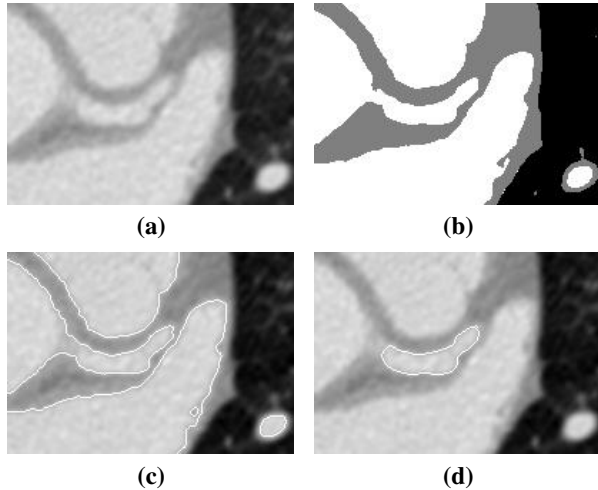


Fig. 2. Segmentation of the left main (LM) coronary artery. (a) The original gray scaled image. (b) Classification result with MAP labels. (c) Blood region marked with boundaries. (d) Segmented left main coronary artery with marked boundaries

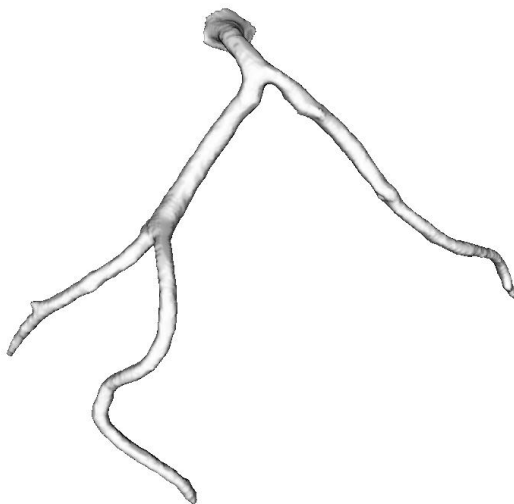


Fig. 3. 3D rendering of the reconstructed left coronary arteries

Future work involves measuring clinically significant parameters from the 3D models, such as the diameters and cross-sectional areas of vessels at different locations, so that a quantitative estimation of stenoses or aneurysms can be provided. We would also need a way of validating the segmentation algorithm by comparing these parameters obtained from the computer generated models either with the results of manual segmentation, or a real cast of vessels.

ACKNOWLEDGMENT

The authors would like to thank Dr. James Gruden at Emory Department of Radiology for providing the CT images used

in this work.

REFERENCES

- [1] L. Antiga, B. Ene-Iordache, L. Caverni, G. P. Cornalba, A. Remuzzi, "Geometric Reconstruction for Computational Mesh Generation of Arterial Bifurcations from CT angiography," *Computerized Medical Imaging and Graphics* **26** (2002), pp. 227-235.
- [2] M. Hernandez, A. F. Frangi, G. Sapiro, "Three-Dimensional Segmentation of Brain Aneurysms in CTA Using Non-parametric Region-Based Information and Implicit Deformable Models: Method and Evaluation", *MICCAI 2003*, LNCS **2879**, pp. 594-602.
- [3] S. D. Olabarriga, M. Breeuwer, W. J. Niessen, "Minimum Cost Path Algorithm for Coronary Artery Central Axis Tracking in CT Images," *MICCAI 2003*, LNCS **2879**, pp. 687-694.
- [4] S. Haker, G. Sapiro, A. Tannenbaum, "Knowledge-Based Segmentation of SAR Data with learned Priors", *IEEE Tran. on Image Processing*, **9** (2000), pp. 298-302.
- [5] P. C. Teo, G. Sapiro, "Creating Connected Representations of Cortical Gray Matter for Functional MRI Visualization," *IEEE Trans. on Medical Imaging* **16** (1997).
- [6] P. Olver, G. Sapiro, and A. Tannenbaum, "Invariant geometric evolutions of surfaces and volumetric smoothing", *SIAM J. Applied Math.* **57** (1997), pp. 176-194.
- [7] S. Kichenassamy, A. Kumar, P. Olver, A. Tannenbaum, and A. Yezzi. "Conformal curvature flows: from phase transitions to active vision," *Archive of Rational Mechanics and Analysis* **134** (1996), pp. 275-301.
- [8] V. Caselles, R. Kimmel, and G. Sapiro. "Geodesic active contours," *Int. Journal Computer Vision*, **22(1)** (1997), pp. 61-79
- [9] A. Yezzi, S. Kichenassamy, A. Kumar, P. Olver, and A. Tannenbaum, "A geometric snake model for segmentation of medical imagery," *IEEE Trans. on Medical Imaging* **16** (1997), pp. 199-209.
- [10] J. Suo, Y. Yang, J. Oshinski, A. Tannenbaum, J. Gruden, D. P. Giddens, "Flow Patterns and Wall Shear Stress Distributions at Atherosclerotic-Prone Sites in a Human Left Coronary Artery - An Exploration Using Combined Methods of CT and Computational Fluid Dynamics", *IEEE EMBS Proceedings*, 2004, submitted.